COMPARISON OF QUASI–ISOTROPIC APPROXIMATIONS OF THE COUPLING RAY THEORY WITH THE EXACT SOLUTION IN THE 1-D ANISOTROPIC "OBLIQUE TWISTED CRYSTAL" MODEL

P. Bulant and L. Klimeš

Department of Geophysics, Faculty of Mathematics and Physics, Charles University, Ke Karlovu 3, 121 16 Praha 2, Czech Republic
(bulant@seis.karlov.mff.cuni.cz, klimes@seis.karlov.mff.cuni.cz)

Received: April 30, 2003; Revised: November 27, 2003; Accepted: December 4, 2003

ABSTRACT

The coupling ray theory bridges the gap between the isotropic and anisotropic ray theories, and is considerably more accurate than the anisotropic ray theory. The coupling ray theory is often approximated by various quasi–isotropic approximations.

Commonly used quasi–isotropic approximations of the coupling ray theory are discussed. The exact analytical solution for the plane S wave, propagating along the axis of spirality in the 1-D anisotropic "oblique twisted crystal" model, is then numerically compared with the coupling ray theory and its three quasi–isotropic approximations. The three quasi–isotropic approximations of the coupling ray theory are (a) the quasi–isotropic projection of the Green tensor, (b) the quasi–isotropic approximation of the Christoffel matrix, (c) the quasi–isotropic perturbation of travel times. The comparison is carried out numerically in the frequency domain, comparing the exact analytical solution with the results of the 3-D ray tracing and coupling ray theory software. In the oblique twisted crystal model, the three studied quasi–isotropic approximations considerably increase the error of the coupling ray theory. Since these three quasi–isotropic approximations do not noticeably simplify the numerical implementation of the coupling ray theory, they should definitely be avoided. The common ray approximations of the coupling ray theory do not affect the plane wave, propagating along the axis of spirality in the 1-D oblique twisted crystal model, and should be studied in more complex models.

Keywords: coupling ray theory, quasi–isotropic approximation, seismic anisotropy, travel time, amplitude, Green tensor

1. INTRODUCTION

There are two different high–frequency asymptotic ray theories: the *isotropic ray theory* assuming equal velocities of both S–wave polarizations and the *anisotropic ray theory* assuming both S–wave polarizations strictly decoupled. In the isotropic ray theory, the S–wave polarization vectors do not rotate about the ray, whereas in the anisotropic ray theory they coincide with the eigenvectors of the Christoffel matrix which may rotate rapidly about the ray. *Thomson, Kendall and Guest (1992)* demonstrated analytically that the high–frequency asymptotic error of the anisotropic ray theory is inversely proportional to the second or higher root of the frequency if a ray passes through the point of equal S–wave eigenvalues of the Christoffel matrix.

In "weakly anisotropic" models, at moderate frequencies, the S–wave polarization tends to remain unrotated round the ray but is partly attracted by the rotation of the eigenvectors of the Christoffel matrix. The intensity of the attraction increases with frequency. The isotropic and anisotropic ray theories are thus limiting cases and the gap between them has to be filled. A ray theory providing continuous transition between the isotropic and anisotropic ray theories was proposed by *Coates and Chapman (1990)* and is called the *coupling ray theory*. A numerical algorithm for calculating the frequency–dependent complex–valued S–wave polarization vectors of the coupling ray theory has been proposed by *Bulant and Klimeš (2002)*. For a brief summary of the method refer to Section 2.

There are many possible modifications and approximations of the coupling ray theory. For example, the reference ray may be calculated in different ways (*Bakker, 2002*), the Christoffel matrix may be approximated by its quasi–isotropic projections onto the plane perpendicular to the reference ray and onto the line tangent to the reference ray (*Pšenčík, 1998*), travel times corresponding to the anisotropic ray theory may be approximated in several ways, e.g., by linear quasi–isotropic perturbation with respect to the density–normalized elastic moduli (*Pšenčík, 1998*), etc. Commonly used quasi–isotropic approximations of the coupling ray theory are discussed in Section 3.

The results of the isotropic ray theory, anisotropic ray theory and coupling ray theory have been compared with the exact solution in the "simplified twisted crystal" model analytically by *Klimeš (2004)* and numerically by *Bulant, Klimeš and Pšenčík (1999; 2000)* and *Bulant et al. (2004)*. The coupling ray theory has been numerically compared with the isotropic ray theory, anisotropic ray theory and reflectivity method in a more realistic 1-D model by *Pšenčík and Dellinger (2001)*.

The effects of the anisotropic common ray approximation by *Bakker (2002)* and the less accurate isotropic common ray approximation are studied by *Klimeš and Bulant (2004)*. The effect of the quasi–isotropic projection of the Green tensor has been numerically demonstrated by *Bulant and Klimeš (2002)* on the example of synthetic seismograms calculated by the coupling ray theory in a 1-D anisotropic model.

The effects of the quasi–isotropic approximation of the Christoffel matrix, the quasi–isotropic projection of the Green tensor and the quasi–isotropic perturbation

of travel times are numerically demonstrated in this paper. In Section 4, a simple 1-D anisotropic "oblique twisted crystal" model is introduced, and the exact solution for the one–way plane–wave propagator matrix is briefly summarized. The numerical results of the coupling ray theory and of its above–mentioned quasi–isotropic approximations are then compared with the exact solution in Section 5.

The lower–case subscripts take values $i, j, k, ... = 1, 2, 3$, the upper–case subscripts take values $I, J, K, ... = 1, 2$; the Einstein summation over pairs of identical indices is applied.

2. COUPLING RAY THEORY FOR S WAVES

Assume a *reference ray* in phase space, parametrized by reference travel time τ, with reference slowness vectors $p_i(\tau)$ known at all its points $x_j(\tau)$. The reference ray should be close to the ray of the wave under study. From the point of view of high–frequency asymptotic validity, the frequency–independent reference ray is best represented by the anisotropic–ray–theory ray, provided we choose the initial condition for the polarization vector in the coupling equation given by the eigenvector of the Christoffel matrix corresponding to the reference ray. Then the anisotropic–ray–theory travel time corresponding to the selected polarization is exact, and only the difference between the two anisotropic–ray–theory S–wave travel times is approximate. The coupling ray theory may then also be used at high frequencies, because the approximate travel–time difference influences only the coupling due to low–frequency scattering.

Using the reference slowness vectors, we can calculate reference Christoffel matrix

$$\Gamma_{jk}(\tau) = p_i(\tau)\, a_{ijkl}(x_m(\tau))\, p_l(\tau) \tag{1}$$

and its eigenvectors $g_{i1}(\tau)$, $g_{i2}(\tau)$, $g_{i3}(\tau)$ along the reference ray. Assume that eigenvectors $g_{i1}(\tau)$ and $g_{i2}(\tau)$ correspond to S waves and that they vary continuously along the reference ray. Continuity is not required in regions where the corresponding two eigenvalues are equal. Let us denote by $\tau_1(\tau)$ and $\tau_2(\tau)$ the travel times corresponding to polarizations $g_{i1}(\tau)$ and $g_{i2}(\tau)$, respectively. They may be approximated by quadratures along the unperturbed reference ray,

$$\frac{\mathrm{d}\tau_1}{\mathrm{d}\tau} = [\Gamma_{jk} g_{j1} g_{k1}]^{-\frac{1}{2}} \quad , \qquad \frac{\mathrm{d}\tau_2}{\mathrm{d}\tau} = [\Gamma_{jk} g_{j2} g_{k2}]^{-\frac{1}{2}} \quad . \tag{2}$$

The coupling–ray–theory solution u_i of the elastodynamic equations may then be expressed, for S waves, as the linear combination

$$u_i = \sum_{M=1}^{2} A\, g_{iM}\, a_M \exp(\mathrm{i}\omega\overline{\tau}) \tag{3}$$

of the anisotropic–ray–theory solutions, where

$$\overline{\tau}(\tau) = \tfrac{1}{2}[\tau_1(\tau) + \tau_2(\tau)] \tag{4}$$

is the average travel time, and $A = A(\tau)$ is the complex–valued scalar amplitude in the high–frequency approximation (*Červený, 1972*), corresponding to the system

of reference rays. The coupling–ray–theory (*Coates and Chapman, 1990*) equation for complex–valued amplitude factors $a_M = a_M(\tau)$ reads (*Bulant and Klimeš, 2002,* eq. 9)

$$\frac{\mathrm{d}}{\mathrm{d}\tau}\begin{pmatrix} a_1 \\ a_2 \end{pmatrix} = \left[\begin{pmatrix} 0 & 1 \\ -1 & 0 \end{pmatrix}\frac{\mathrm{d}\varphi}{\mathrm{d}\tau} + \begin{pmatrix} \mathrm{i} & 0 \\ 0 & -\mathrm{i} \end{pmatrix}\frac{\omega}{2}\frac{\mathrm{d}(\tau_1-\tau_2)}{\mathrm{d}\tau}\right]\begin{pmatrix} a_1 \\ a_2 \end{pmatrix} \quad , \tag{5}$$

where

$$\frac{\mathrm{d}\varphi}{\mathrm{d}\tau} = \frac{\mathrm{d}g_{k1}}{\mathrm{d}\tau}\, g_{k2} = -g_{k1}\frac{\mathrm{d}g_{k2}}{\mathrm{d}\tau} \tag{6}$$

is the angular velocity of the eigenvector rotation.

2.1. Coupling–ray–theory S–wave propagator matrix

Propagator matrix Π^g of equation (5), defined as

$$\Pi^g_{MN}(\tau,\tau_0) = \frac{\partial\, a_M(\tau)}{\partial\, a_N(\tau_0)} \quad , \tag{7}$$

is a complex–valued 2×2 matrix satisfying equation (*Bulant and Klimeš, 2002,* eq. 11)

$$\frac{\mathrm{d}}{\mathrm{d}\tau}\Pi^g = \left[\begin{pmatrix} 0 & 1 \\ -1 & 0 \end{pmatrix}\frac{\mathrm{d}\varphi}{\mathrm{d}\tau} + \begin{pmatrix} \mathrm{i} & 0 \\ 0 & -\mathrm{i} \end{pmatrix}\frac{\mathrm{d}\psi}{\mathrm{d}\tau}\right]\Pi^g \quad , \tag{8}$$

directly following from equation (5). Here

$$\psi(\tau) = \tfrac{1}{2}\omega\,[\tau_1(\tau) - \tau_2(\tau)] \quad . \tag{9}$$

Note that propagator matrix Π^g is symplectic and unitary.

It is difficult to integrate equation (8) by the Runge–Kutta or another numerical method that requires derivative $\frac{\mathrm{d}\varphi}{\mathrm{d}\tau}$ along the reference ray to be calculated, because this derivative is undefined in the singular regions of the two equal eigenvalues of Christoffel matrix (1). The method of calculating propagator matrix Π^g, fit for equation (8), has been proposed by *Červený (2001)* and *Bulant and Klimeš (2002)*, with emphasis on numerical implementation. The method does not require the calculation of the angular velocity $\frac{\mathrm{d}\varphi}{\mathrm{d}\tau}$ of the rotation of the eigenvectors of the Christoffel matrix along the reference ray and does not require $\frac{\mathrm{d}\varphi}{\mathrm{d}\tau}$ to be smooth or finite along the reference ray. This is an important property, because the angular velocity of the rotation is undefined in the singular regions of the two equal eigenvalues of the Christoffel matrix.

The proposed method of solving equation (8) takes advantage of the chain rule. Since Π^g is a propagator matrix satisfying the chain rule, it may be numerically calculated as the product of propagator matrices Π^g corresponding to reasonably small segments of the reference ray (*Červený, 2001*). Frequency–dependent propagator matrices along the individual small ray segments may be approximated by the method of mean coefficients (*Červený, 2001*). The accuracy of the proposed algorithm of numerical integration of the coupling equation has been estimated by

Bulant and Klimeš (2002) in order to control the integration step, so that the relative error in the wavefield amplitudes due to the integration is kept below a given limit, which is of principal importance for numerical applications.

The calculation of P–wave travel–time perturbations from a reference isotropic model to an anisotropic model and the calculation of the S–wave coupling–ray–theory travel–time and amplitude corrections along isotropic reference rays have been coded and added to the Fortran 77 package CRT (*Bucha and Bulant, 2002*).

3. QUASI–ISOTROPIC APPROXIMATIONS OF THE COUPLING RAY THEORY

The coupling ray theory by *Coates and Chapman (1990)* is applicable at all degrees of anisotropy, but it is often modified by various *quasi–isotropic approximations*.

3.1. Selection of the reference ray

The isotropic ray theory is always the limiting case of the coupling ray theory for decreasing anisotropy at a fixed frequency. On the other hand, the high–frequency limit of the coupling ray theory at a fixed anisotropy depends on the choice of the reference ray, and even on the choice of the *system* of reference rays, because the amplitudes are determined by the paraxial reference rays.

If we choose the *anisotropic–ray–theory reference ray* and select the initial condition for the polarization vector in the coupling equation given by the eigenvector of the Christoffel matrix corresponding to the reference ray, the coupling ray theory will correctly converge to the anisotropic ray theory for high–frequencies. For other choices of reference rays, the high–frequency limit of the coupling ray theory at a fixed anisotropy is incorrect, although the differences may be small at the finite frequencies under consideration.

In the *anisotropic common ray approximation*, the common reference ray is traced using the averaged Hamiltonian of both anisotropic–ray-theory S waves (*Bakker, 2002*; *Klimeš, 2003*). This is probably the best common ray approximation (*Klimeš and Bulant, 2004*).

In the less accurate *isotropic common ray approximation*, the reference ray is traced in the reference isotropic model. Moreover, the reference isotropic model may be selected in different ways, yielding quasi–isotropic approximations of differing accuracies.

A method of estimating the errors due to the isotropic common ray approximation and anisotropic common ray approximation has been proposed by *Klimeš and Bulant (2004)*. The method is based on the equations for the second–order perturbations of travel time derived by *Klimeš (2002)*.

3.2. Quasi–isotropic projection of the Green tensor

The coupling–ray–theory solution (3) may be approximated by its projection

$$\tilde{u}_i = h_{iM} h_{mM} u_m \tag{10}$$

onto the reference S–wave polarization plane, given by two orthonormal reference polarization vectors h_{k1}, h_{k2}. This approximation may simplify the modification of existing isotropic ray tracing codes for the coupling ray theory, and has been used by *Bucha, Bulant and Klimeš (2001)* and by *Bulant and Klimeš (2002)*. The error of this approximation is obvious and simple to calculate.

3.3. Quasi–isotropic approximation of the Christoffel matrix

The Christoffel matrix may be approximated by its projections onto the reference S–wave polarization plane and onto the reference P–wave polarization line. Denote the polarization vectors of the isotropic ray theory, or the reference polarization vectors in general, by h_{k1}, h_{k2} and h_{k3}. If the Christoffel matrix is approximated by its projections onto plane h_{j1}, h_{k2} and onto vector h_{l3}, namely,

$$\begin{aligned}\tilde{\Gamma}_{jk} &= h_{jM} h_{mM} \Gamma_{mn} h_{nN} h_{kN} + h_{j3} h_{m3} \Gamma_{mn} h_{n3} h_{k3} \\ &= \Gamma_{jk} - (h_{jM} h_{k3} + h_{j3} h_{kM}) h_{mM} \Gamma_{mn} h_{n3} \quad ,\end{aligned} \tag{11}$$

then eigenvectors g_{k1} and g_{k2} become located in plane h_{j1}, h_{k2} as in the zero-order quasi–isotropic approximation of *Pšenčík (1998)*. This approximation includes the quasi–isotropic projection of the Green tensor described in Section 3.2.

The quasi–isotropic approximation of the Christoffel matrix is probably the worst quasi–isotropic approximation. The alteration of the coupling–ray–theory synthetic seismograms due to the quasi–isotropic approximation of the Christoffel matrix has been demonstrated by *Bulant and Klimeš (2002)*.

3.4. Quasi–isotropic perturbation of travel times

The anisotropic–ray–theory travel times used in the coupling ray theory should be calculated by the numerical quadrature of equations (2) along the reference ray. In the quasi–isotropic perturbation of travel times, the anisotropic–ray–theory travel times are calculated from the reference travel time by the linear perturbation with respect to the density–normalized elastic moduli,

$$\frac{\mathrm{d}\tau_1}{\mathrm{d}\tau} \approx (\Gamma^0_{jk} g_{j1} g_{k1})^{-\frac{1}{2}} - \frac{1}{2} (\Gamma_{jk} - \Gamma^0_{jk}) g_{j1} g_{k1} (\Gamma^0_{jk} g_{j1} g_{k1})^{-\frac{3}{2}} \quad . \tag{12}$$

Assuming that

$$\Gamma^0_{jk} g_{j1} g_{k1} = 1 \quad , \tag{13}$$

see Section 3.3, equation (12) becomes

$$\frac{\mathrm{d}\tau_1}{\mathrm{d}\tau} \approx \frac{3}{2} - \frac{1}{2}\Gamma_{jk} g_{j1} g_{k1} \quad , \tag{14}$$

as in the quasi–isotropic approximation of *Pšenčík (1998)*. Analogously, we obtain $\frac{\mathrm{d}\tau_2}{\mathrm{d}\tau}$. The quasi–isotropic perturbation of travel times leads to an erroneous time shift in synthetic seismograms but has a negligible impact on the amplitudes.

4. TWISTED CRYSTAL MODELS

The *twisted crystal* model is created of a homogeneous anisotropic elastic material by uniformly helicoidally twisting the x_1x_2 coordinate plane about the x_3 axis. It is one of the simplest models useful for demonstrating the limits of applicability of the zero–order isotropic and anisotropic ray theories and for testing the coupling ray theory (*Coates and Chapman, 1990*), which is the generalization of both the zero–order isotropic and anisotropic ray theories and provides continuous transition between them.

The great advantage of this model is that the exact analytical solution for the plane S wave propagating along the axis of spirality can be examined analytically (*Lakhtakia, 1994*; *Klimeš, 2004*). The general plane–wave solution for the general initial conditions expressed in terms of displacement and stress was derived by *Lakhtakia (1994)*, who also presented explicit analytical equations for the *simplified twisted crystal model* with vanishing a_{1333} and a_{2333}, in which the u_1 and u_2 displacement components are strictly separated from the longitudinal u_3 component. *Klimeš (2004)* derived the 2×2 one–way propagator matrices in the simplified twisted crystal model, suitable for comparison with the coupling ray theory.

In this paper, we shall modify the simplified twisted crystal model towards the *oblique twisted crystal model* in order to allow the quasi–isotropic approximations of the coupling ray theory to be studied.

The elastodynamic equation in the frequency domain reads

$$(\varrho a_{ijkl} u_{k,l})_{,j} = -\varrho\,\omega^2 u_i \quad , \tag{15}$$

where a_{ijkl} are the density–normalized elastic moduli (stiffness tensor).

For the plane wave $u_i = u_i(x_3)$ propagating along the x_3 axis in the 1-D anisotropic model $a_{ijk3} = a_{ijk3}(x_3)$ with constant density ϱ, elastodynamic equation (15) simplifies to

$$(a_{i3k3} u_{k,3})_{,3} = -\omega^2 u_i \quad . \tag{16}$$

Equation (16) contains only 6 elastic moduli $a_{i3k3} = a_{i3k3}(x_3)$. Due to the separation of plane waves, the 15 remaining elastic moduli a_{ijKL} may arbitrarily depend on x_3. Moreover, the 6 elastic moduli a_{IJKL} may arbitrarily depend on all three spatial coordinates x_i.

4.1. Simplified twisted crystal model

In the 1-D anisotropic *simplified twisted crystal model* we take

$$\overline{a}_{K333} = 0 \quad . \tag{17}$$

Components u_K are then fully separated from u_3. We choose moduli $\overline{a}_{I3K3}$ in the form of

$$\begin{pmatrix} \overline{a}_{1313} & \overline{a}_{1323} & \overline{a}_{1333} \\ \overline{a}_{2313} & \overline{a}_{2323} & \overline{a}_{2333} \\ \overline{a}_{3313} & \overline{a}_{3323} & \overline{a}_{3333} \end{pmatrix} = \begin{pmatrix} v_{\mathrm{S}}^2 B_{11} & v_{\mathrm{S}}^2 B_{12} & 0 \\ v_{\mathrm{S}}^2 B_{21} & v_{\mathrm{S}}^2 B_{22} & 0 \\ 0 & 0 & v_{\mathrm{P}}^2 \end{pmatrix} \tag{18}$$

with the symmetric 2×2 matrix $\mathbf{B}$ defined by

$$\begin{pmatrix} B_{11} & B_{12} \\ B_{21} & B_{22} \end{pmatrix} = \begin{pmatrix} 1+\varepsilon\cos(2Kx_3) & \varepsilon\sin(2Kx_3) \\ \varepsilon\sin(2Kx_3) & 1-\varepsilon\cos(2Kx_3) \end{pmatrix} \quad . \tag{19}$$

Parameter K describes the rotation of the crystal axes about the x_3 axis, parameter ε determines the relative difference between the faster and slower S–wave velocities.

Elastodynamic equation (16) for the plane S wave in the simplified twisted crystal model then reads

$$(\mathbf{B}\mathbf{u}')' = -k_{\mathrm{S}}^2 \mathbf{u} \quad , \tag{20}$$

where the prime denotes the derivative with respect to x_3 and

$$\mathbf{u} = \begin{pmatrix} u_1 \\ u_2 \end{pmatrix} \quad , \quad k_{\mathrm{S}} = \frac{\omega}{v_{\mathrm{S}}} \quad . \tag{21}$$

Elastodynamic equation (16) for the plane P wave in the simplified twisted crystal model reads

$$v_{\mathrm{P}}^2 u_3'' = -\omega^2 u_3 \quad . \tag{22}$$

4.2. Exact analytical solution in the simplified twisted crystal model

The 3×3 one–way propagator matrix $\overline{U}_{ij}$ of elastodynamic equation (16) in the simplified twisted crystal model may be decomposed into its S–wave part U_{ij}^{S} and P–wave part U_{ij}^{P},

$$\overline{U}_{ij} = U_{ij}^{\mathrm{S}} + U_{ij}^{\mathrm{P}} \quad . \tag{23}$$

The S–wave part of the 3×3 one–way propagator matrix reads

$$\begin{pmatrix} U_{11}^{\mathrm{S}} & U_{12}^{\mathrm{S}} & U_{13}^{\mathrm{S}} \\ U_{21}^{\mathrm{S}} & U_{22}^{\mathrm{S}} & U_{23}^{\mathrm{S}} \\ U_{31}^{\mathrm{S}} & U_{32}^{\mathrm{S}} & U_{33}^{\mathrm{S}} \end{pmatrix} = \begin{pmatrix} U_{11}^{\mathrm{S}} & U_{12}^{\mathrm{S}} & 0 \\ U_{21}^{\mathrm{S}} & U_{22}^{\mathrm{S}} & 0 \\ 0 & 0 & 0 \end{pmatrix} \quad , \tag{24}$$

where U_{IJ}^{S} are the components of the 2×2 one–way S–wave propagator matrix $\mathbf{U}^{\mathrm{S}}$ of elastodynamic equation (20) for the plane S wave. The P–wave part of the 3×3 one–way propagator matrix reads

$$\begin{pmatrix} U_{11}^{\mathrm{P}} & U_{12}^{\mathrm{P}} & U_{13}^{\mathrm{P}} \\ U_{21}^{\mathrm{P}} & U_{22}^{\mathrm{P}} & U_{23}^{\mathrm{P}} \\ U_{31}^{\mathrm{P}} & U_{32}^{\mathrm{P}} & U_{33}^{\mathrm{P}} \end{pmatrix} = \begin{pmatrix} 0 & 0 & 0 \\ 0 & 0 & 0 \\ 0 & 0 & U_{33}^{\mathrm{P}} \end{pmatrix} \quad , \tag{25}$$

where U_{33}^{P} is the one–way P–wave propagator of elastodynamic equation (22) for the plane P wave.

The P–wave part of the one–way plane–wave propagator matrix is very simple,

$$U_{33}^{\mathrm{P}} = \exp\left(\pm\frac{\mathrm{i}\omega}{v_{\mathrm{P}}}x_3\right) \quad . \tag{26}$$

The anisotropic ray theory yields this exact solution.

In this paper, we shall study only the S–wave part of the one–way plane–wave propagator matrix. The 2×2 one–way propagator matrix $\mathbf{U}^{\mathrm{S}}$ of elastodynamic equation (20) may be described by four frequency–dependent coefficients F_0, F_1, F_2 and F_3 (*Klimeš, 2004*),

$$\begin{aligned}\mathbf{U}^{\mathrm{S}} = &\exp(\mathrm{i}\mathrm{Re}(F_0)x_3)[\mathbf{1}\cos(Kx_3) - \mathrm{i}\boldsymbol{\sigma}_2\sin(Kx_3)]\\ &\times[\mathbf{1}\cos(\mathrm{Re}(\varphi)x_3) + \mathrm{i}\boldsymbol{\Phi}\sin(\mathrm{Re}(\varphi)x_3)]\\ &\times\exp(-\mathrm{Im}(F_0)x_3)[\mathbf{1}\cosh(\mathrm{Im}(\varphi)x_3) - \boldsymbol{\Phi}\sinh(\mathrm{Im}(\varphi)x_3)],\end{aligned} \tag{27}$$

where $\mathbf{1}$ is the 2×2 identity matrix,

$$\boldsymbol{\Phi} = [F_1\mathrm{i}\boldsymbol{\sigma}_1 + F_2\boldsymbol{\sigma}_2 + F_3\boldsymbol{\sigma}_3]\varphi^{-1} \quad , \tag{28}$$

$$\varphi = \sqrt{F_3^2 + F_2^2 - F_1^2} \tag{29}$$

and

$$\boldsymbol{\sigma}_1 = \begin{pmatrix}0 & 1\\ 1 & 0\end{pmatrix} \quad , \qquad \boldsymbol{\sigma}_2 = \begin{pmatrix}0 & -\mathrm{i}\\ \mathrm{i} & 0\end{pmatrix} \quad , \qquad \boldsymbol{\sigma}_3 = \begin{pmatrix}1 & 0\\ 0 & -1\end{pmatrix} \tag{30}$$

are the Pauli matrices. The exact one–way propagator matrix has coefficients

$$F_1 = \frac{\varepsilon K k_{\mathrm{S}}^2}{(k_{\mathrm{S}}^2 - K^2)\sqrt{1-\varepsilon^2}\left[\sqrt{1-\varepsilon^2} + \sqrt{1-\varepsilon^2\left(\frac{K^2}{k_{\mathrm{S}}^2-K^2}\right)^2}\right]} \quad , \tag{31}$$

$$F_2 = K + \varepsilon F_1 \quad , \tag{32}$$

$$F_3 = F_0\left[-\varepsilon + \frac{F_1(1-\varepsilon^2)}{K}\right] \quad , \tag{33}$$

$$F_0^2 = \left[\frac{k_{\mathrm{S}}^2}{1-\varepsilon^2} + F_1^2\right]\left[1 + \frac{F_1^2(1-\varepsilon^2)}{K^2}\right]^{-1} \quad . \tag{34}$$

The sign of F_0 has to be determined according to the desired direction of the one–way plane–wave propagation and corresponds to the sign of the exponent in equation (26). Two possible signs of F_0 correspond to the two one–way propagator matrices in opposite directions. For example, if the time factor is $\exp(-\mathrm{i}\omega t)$ for positive circular frequencies ω, positive $\mathrm{Re}(F_0)$ corresponds to the propagation in the direction of the positive half–axis x_3, and negative $\mathrm{Re}(F_0)$ to the propagation in the direction of the negative half–axis x_3. For "resonant frequencies" (*Klimeš, 2004,* sec. 3.4; *Lakhtakia and Meredith, 1999,* sec. 3) within domain

$$(1-|\varepsilon|)\,K^2 \le k_{\mathrm{S}}^2 \le (1+|\varepsilon|)\,K^2 \quad , \tag{35}$$

where F_0, F_1, F_2 and F_3 are complex–valued, we may determine F_1 from equation (31), arbitrarily selecting one of the complex–conjugate roots. After inserting into (34) and determining F_0 with its real part corresponding to the desired direction of propagation, we check for the proper sign of the imaginary part of F_0. The imaginary part of F_0 has to compensate the exponential increase of the cosh in equation (27). That is why $\mathrm{Im}(F_0)$ should be positive for propagation in the direction of the positive half–axis x_3 and negative for propagation in the direction of the negative half–axis x_3, independently of time factor $\exp(\pm \mathrm{i}\omega t)$. If the imaginary part does not correspond to the direction of propagation, we replace F_0 and F_1 by their complex–conjugates. Equations (32), (33) and (27) are then used as they are.

4.3. Oblique twisted crystal model

In the simplified twisted crystal model, S–wave polarization vectors g_{iM} of the anisotropic ray theory are situated in the same plane as the reference S–wave polarization vectors, see equations (10) and (11). Then neither the quasi–isotropic projection of the Green tensor, nor the quasi–isotropic approximation of the Christoffel matrix has any impact on the results of the coupling ray theory. We thus modify the model in order to demonstrate these quasi–isotropic approximations.

In the *oblique twisted crystal model*, we select elastic moduli

$$a_{i3k3} = E_{im} E_{kn} \overline{a}_{m3n3} \quad , \tag{36}$$

where E_{im} are the components of a constant 3×3 real–valued orthogonal matrix. Elastic moduli $\overline{a}_{i3k3}$, corresponding to the simplified twisted crystal model, are given by (18). For the specification of real–valued orthogonal matrix E_{im} in terms of rotation vector E_i refer to the Appendix.

4.4. Exact analytical solution in the oblique twisted crystal model

The exact 3×3 one–way propagator matrix U_{ij} of elastodynamic equation (16) in the oblique twisted crystal model is

$$U_{ij} = E_{im} E_{jn} \overline{U}_{mn} \quad , \tag{37}$$

where $\overline{U}_{mn}$ are the components of the 3×3 one–way propagator matrix (23) in the simplified twisted crystal model. Indeed, elastodynamic equation (16) with elastic moduli (36) and one–way propagator matrix (37) is equivalent to the same equation with elastic moduli $\overline{a}_{i3k3}$ and one–way propagator matrix $\overline{U}_{ij}$.

5. NUMERICAL COMPARISON WITH THE EXACT SOLUTION

For the numerical comparison, we define the relative (with respect to the initial conditions) difference between one–way propagator matrices $\mathbf{U}^{\mathrm{S}}$ and $\mathbf{U}_0^{\mathrm{S}}$ as

$$\Delta = \sqrt{\tfrac{1}{2}\mathrm{tr}\Big([\mathbf{U}_0^{\mathrm{S}} - \mathbf{U}^{\mathrm{S}}]^{+}[\mathbf{U}_0^{\mathrm{S}} - \mathbf{U}^{\mathrm{S}}]\Big)} \quad , \tag{38}$$

where $\mathbf{U}^{+}$ denotes the matrix Hermitian adjoined to $\mathbf{U}$.

5.1. Model for the numerical comparison

We use the simplified twisted crystal model designed by *Vavryčuk (1999)*. The relation to *Vavryčuk*'s *(1999)* notation is

$$\varepsilon = \frac{-\gamma \sin^2(\vartheta)}{1+\gamma \sin^2(\vartheta)} \quad , \qquad v_{\mathrm{S}}^2 = a_{44}[1+\gamma \sin^2(\vartheta)] \quad , \qquad Kx_3 = \varphi \quad . \tag{39}$$

The selected numerical values in (39) are

$$\gamma \sin^2(\vartheta) = 0.15 \times 0.75 = 0.1125 \quad , \tag{40}$$

$$v_{\mathrm{S}}^2 = 6.0\,\mathrm{km^2 s^{-2}} \times [1 + 0.15 \times 0.75] = 6.675\,\mathrm{km^2 s^{-2}} \quad . \tag{41}$$

The relative difference between the faster and slower S–wave velocities is thus about 10%. Parameter K describing the rotation of the crystal axes about the x_3 axis has the value

$$K = 0.032\,\mathrm{km^{-1}} \quad . \tag{42}$$

The source–receiver distance corresponds to the crystal axes rotated by $\varphi = \pi$ radians,

$$x_3 = \frac{\pi}{K} \approx 98.17477\,\mathrm{km} \quad . \tag{43}$$

The *central resonant frequency*, see (35), is

$$F = \left| \frac{v_{\mathrm{S}} K}{2\pi} \right| \approx 0.0132\,\mathrm{Hz} \tag{44}$$

and the *coupling frequency* (*Klimeš, 2004*, section 4.2) is

$$\left| \frac{2}{\varepsilon} \right| F \approx 0.260\,\mathrm{Hz} \quad . \tag{45}$$

The squared P–wave velocity in (18) is

$$v_{\mathrm{P}}^2 = 3 v_{\mathrm{S}}^2 \quad . \tag{46}$$

The rotation vector (see Section 4.3 and Appendix) for the oblique twisted crystal model is

$$E_1 = 0.10 \quad , \qquad E_2 = 0 \quad , \qquad E_3 = 0 \quad . \tag{47}$$

The rotation angle (0.10 radians) thus roughly corresponds to the strength of the anisotropy (10% difference between the S–wave velocities).

5.2. Numerical results

The approximate 3×3 one–way propagator matrices of the plane S wave, corresponding to the coupling ray theory and its quasi–isotropic approximations, have been numerically calculated by means of the Fortran 77 package CRT (*Bucha and Bulant, 2002*). The relative differences of the coupling ray theory, its quasi–isotropic approximations and their combinations from the exact analytical solution are plotted on a log–log scale in Figure 1.

The coupling ray theory of *Coates and Chapman (1990)* yields excellent results in this model, except for the resonant frequencies, which are far outside the validity regions of the ray theories. On the other hand, the quasi–isotropic approximations applied here generate unnecessary additional errors and should be avoided when using the coupling ray theory.

The error of the *quasi–isotropic projection of the Green tensor* (Section 3.2) can be estimated simply. It is frequency–independent, and corresponds to the rotation angle in this model, see (47). This frequency–independent error may be expected to be roughly proportional to the degree of anisotropy in generally anisotropic models.

The *quasi–isotropic approximation of the Christoffel matrix* (Section 3.3) generates the travel–time error. The wavefield error is then proportional to the frequency. The error is proportional to the square of the angle between the correct S–wave polarization plane and the reference S–wave polarization plane (to the square of the rotation angle in the oblique twisted crystal model). The wavefield error, proportional to the frequency, may thus be expected to be proportional to the square of the degree of anisotropy in generally anisotropic models on average. The quasi–isotropic approximation of the Christoffel matrix seems to be the worst quasi–isotropic approximation.

The *quasi–isotropic perturbation of travel times* (Section 3.4) generates the travel–time error. The wavefield error is then proportional to the frequency. The error is proportional to the square of the difference between the anisotropic model and the reference isotropic model. The quasi–isotropic perturbation of travel times thus depends on the reference velocity. The wavefield error, proportional to the frequency, may be expected to be proportional to the square of the degree of anisotropy in generally anisotropic models on average.

The *common ray approximations* (Section 3.1) have no impact on the coupling ray theory in this model. The inaccuracy due to the common ray approximations is studied by *Klimeš and Bulant (2004)*.

The behaviour of the errors due to the quasi–isotropic approximations of the coupling ray theory when decreasing rotation angle E_1 in (47) towards the simplified twisted crystal model, used for comparison with the isotropic ray theory and anisotropic ray theory by *Bulant et al. (1999; 2000; 2004)*, is demonstrated in Figures 2 to 5.

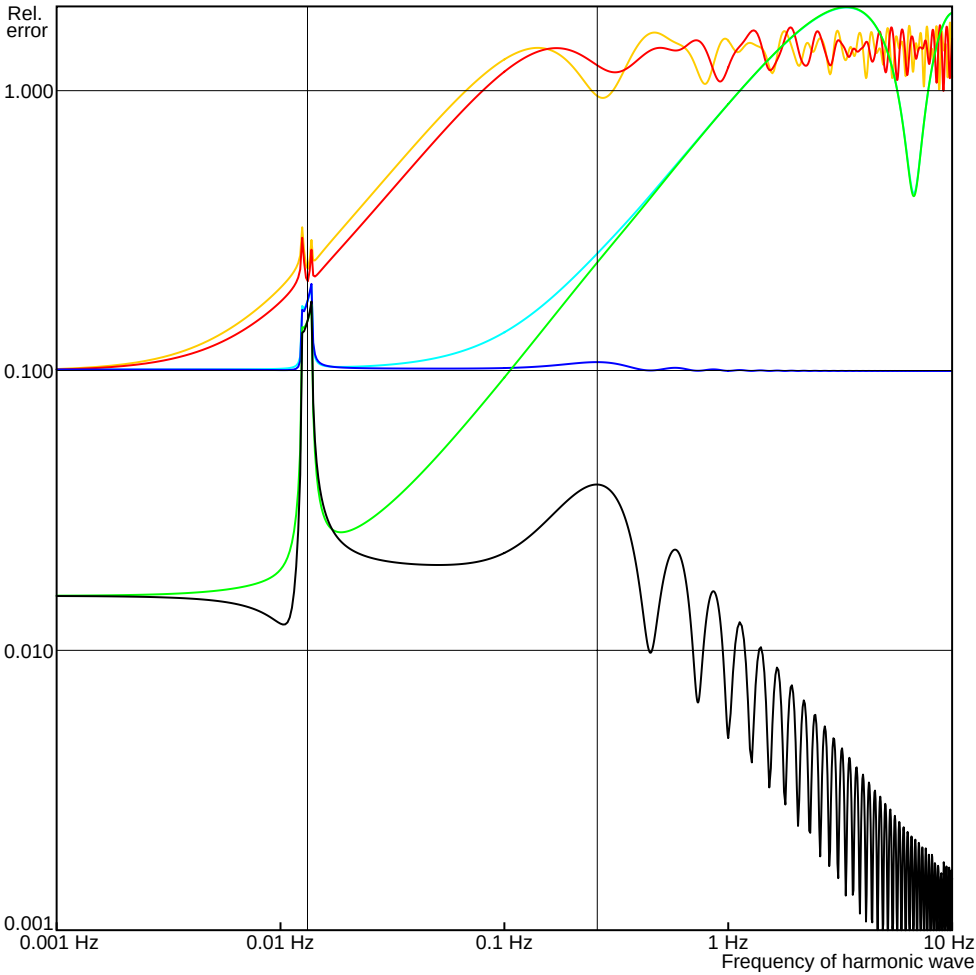

Fig. 1. The relative differences of various approximations of the coupling ray theory (*Coates and Chapman, 1990*) from the exact solution in the oblique twisted crystal model. **Black**: No quasi–isotropic approximation. **Blue**: Quasi–isotropic projection of the Green tensor. **Red**: Quasi–isotropic approximation of the Christoffel matrix. This includes the quasi–isotropic projection of the Green tensor. **Green**: Quasi–isotropic perturbation of travel times with the best reference velocity (41). **Cyan**: Quasi–isotropic projection of the Green tensor combined with the quasi–isotropic perturbation of travel times. **Yellow**: Quasi–isotropic approximation of the Christoffel matrix combined with the quasi–isotropic perturbation of travel times. The two vertical lines denote the central resonant and coupling frequencies (44), (45). The relative error of 200% occurs, e.g., for an opposite polarization or an opposite phase.

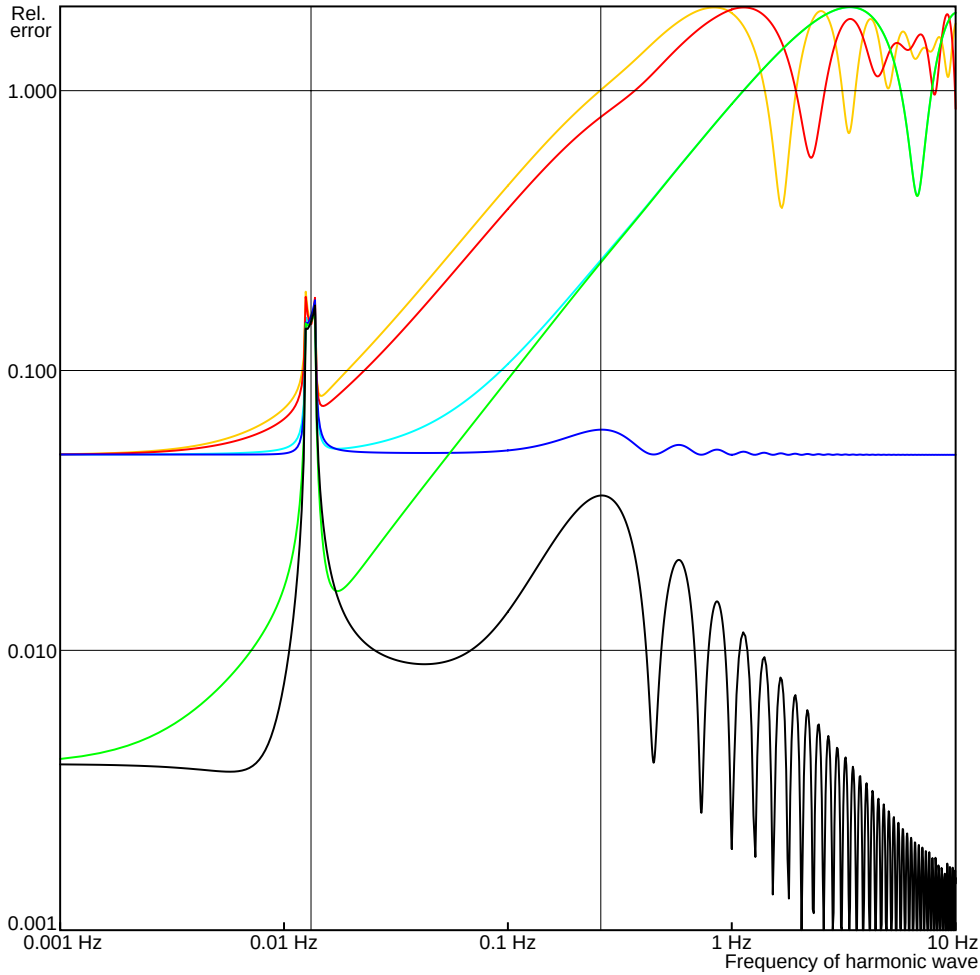

Fig. 2. Analogous to Figure 1, but for a different oblique twisted crystal model obtained by modifying rotation angle E_1 in data (47). Whereas the model for Figure 1 is given by $E_1 = 0.10$, the differences plotted here correspond to $E_1 = 0.05$.

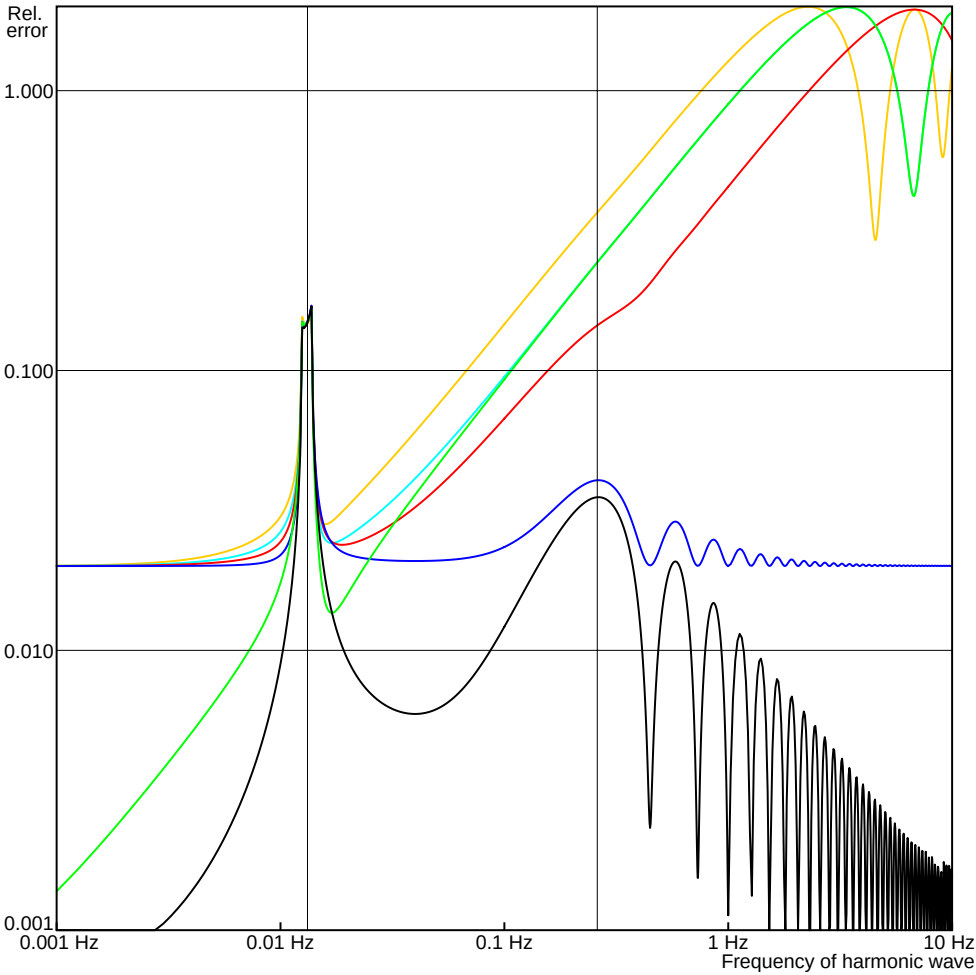

Fig. 3. Analogous to Figure 1, but for a different oblique twisted crystal model obtained by modifying rotation angle E_1 in data (47). Whereas the model for Figure 1 is given by $E_1 = 0.10$, the differences plotted here correspond to $E_1 = 0.02$.

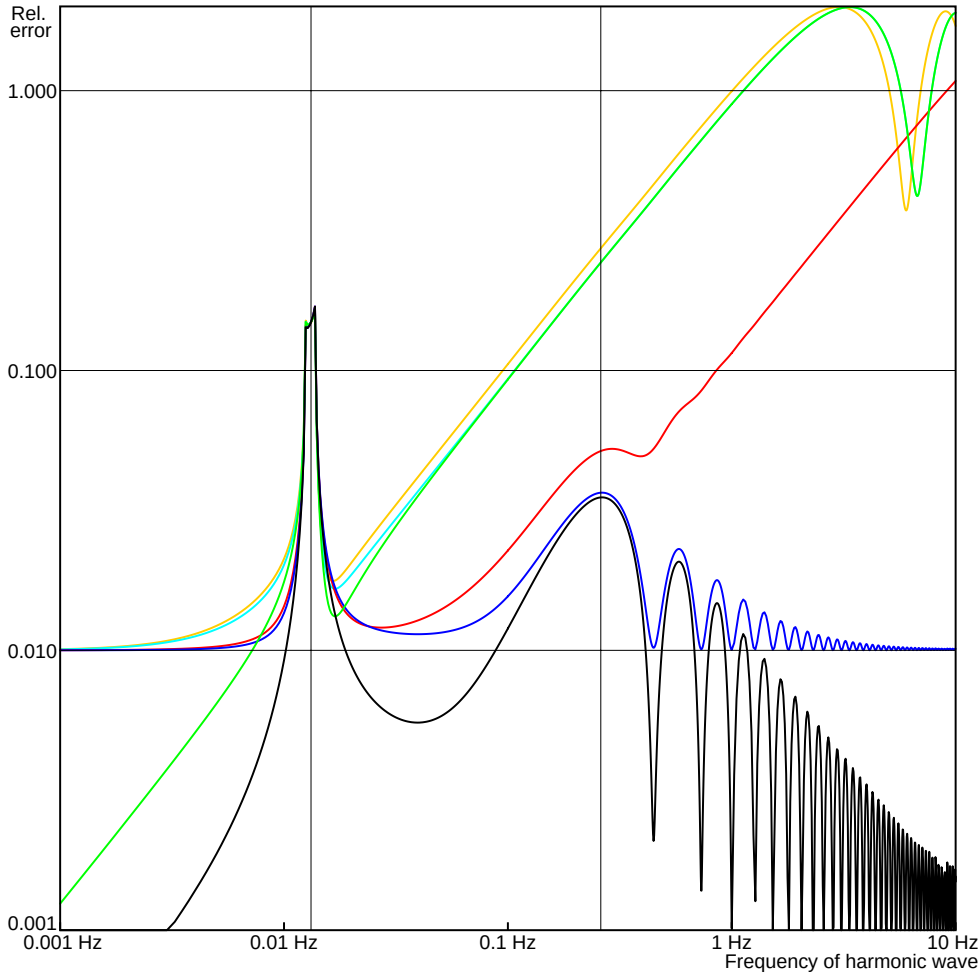

Fig. 4. Analogous to Figure 1, but for a different oblique twisted crystal model obtained by modifying rotation angle E_1 in data (47). Whereas the model for Figure 1 is given by $E_1 = 0.10$, the differences plotted here correspond to $E_1 = 0.01$.

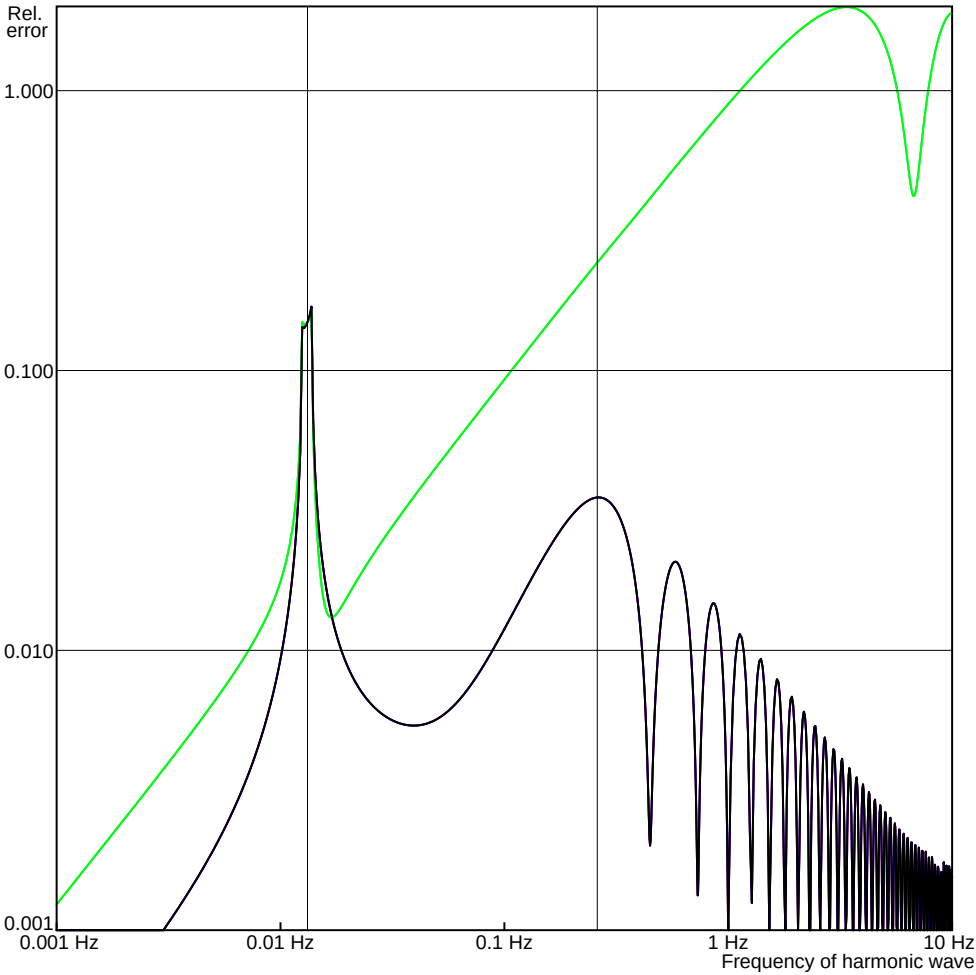

Fig. 5. Analogous to Figure 1, but for the simplified twisted crystal model obtained by modifying rotation angle E_1 in data (47). Whereas the model for Figure 1 is given by $E_1 = 0.10$, the differences plotted here correspond to $E_1 = 0.00$. Only the quasi–isotropic perturbation of travel times can be demonstrated in the simplified twisted crystal model.

6. CONCLUSIONS

The common quasi–isotropic approximations of the coupling ray theory are listed in Section 3. We have compared the exact analytical solution of the elastodynamic equation in the oblique twisted crystal model with the coupling ray theory and its three quasi–isotropic approximations, see Figures 1 to 5. The three quasi–isotropic approximations of the coupling ray theory are (a) the quasi–isotropic projection of the Green tensor, (b) the quasi–isotropic approximation of the Christoffel matrix, (c) the quasi–isotropic perturbation of travel times. In the oblique twisted crystal model, the three studied quasi–isotropic approximations considerably increase the error of the coupling ray theory. Since these three quasi–isotropic approximations do not noticeably simplify the numerical implementation of the coupling ray theory, they should definitely be avoided. Although the oblique twisted crystal model is designed for testing purposes and has no direct relation to geological structures, the wave–propagation phenomena important in the comparison are similar to those in the models of geological structures.

The common ray approximations of the coupling ray theory (Section 3.1) do not affect the plane wave propagating along the axis of spirality in the 1-D oblique twisted crystal model. The errors due to the common ray approximations are studied by *Klimeš and Bulant (2004)*.

For additional information, including electronic reprints, computer codes and data, refer to the consortium research project "Seismic Waves in Complex 3-D Structures" ("http://sw3d.mff.cuni.cz").

Acknowledgements: The authors are grateful to Ivan Pšenčík and two anonymous reviewers whose comments enabled the improvement of this paper.

The research has been supported by the Grant Agency of the Czech Republic under Contracts 205/01/0927, 205/01/D097 and 205/04/1104, by the Grant Agency of the Charles University under Contracts 237/2001/B-GEO/MFF and 229/2002/B-GEO/MFF, by the Ministry of Education of the Czech Republic within Research Project MSM113200004, and by the members of the consortium "Seismic Waves in Complex 3-D Structures" (see "http://sw3d.mff.cuni.cz").

References

Bakker, P.M., 2002. Coupled anisotropic shear wave raytracing in situations where associated slowness sheets are almost tangent. *Pure Appl. Geophys.*, **159**, 1403–1417.

Bucha, V. and Bulant, P. (eds.), 2002. SW3D–CD–6 (CD–ROM). In: *Seismic Waves in Complex 3-D Structures, Report 12*, pp. 247–247, Dep. Geophys., Charles Univ., Prague, online at "http://sw3d.mff.cuni.cz".

Bucha, V., Bulant, P. and Klimeš, L. (eds.), 2001. SW3D–CD–5 (CD–ROM). In: *Seismic Waves in Complex 3-D Structures, Report 11*, pp. 357–357, Dep. Geophys., Charles Univ., Prague, online at "http://sw3d.mff.cuni.cz".

Bulant, P. and Klimeš, L., 2002. Numerical algorithm of the coupling ray theory in weakly anisotropic media. *Pure Appl. Geophys.*, **159**, 1419–1435.

Bulant, P., Klimeš, L. and Pšenčík, I., 1999. Comparison of ray methods with the exact solution in the 1-D anisotropic "twisted crystal" model. In: *Seismic Waves in Complex 3-D Structures, Report 8*, pp. 119–126, Dep. Geophys., Charles Univ., Prague, online at "http://sw3d.mff.cuni.cz".

Bulant, P., Klimeš, L. and Pšenčík, I., 2000. Comparison of ray methods with the exact solution in the 1-D anisotropic "twisted crystal" model. In: *Expanded Abstracts of 70th Annual Meeting (Calgary)*, pp. 2289–2292, Soc. Explor. Geophysicists, Tulsa.

Bulant, P., Klimeš, L., Pšenčík, I. and Vavryčuk, V., 2004. Comparison of ray methods with the exact solution in the 1-D anisotropic "simplified twisted crystal" model. *Stud. Geophys. Geod.*, **48**, in press.

Červený, V., 2001. *Seismic Ray Theory.* Cambridge Univ. Press, Cambridge.

Coates, R.T. and Chapman, C.H., 1990. Quasi–shear wave coupling in weakly anisotropic 3-D media. *Geophys. J. Int.*, **103**, 301–320.

Klimeš, L., 2002. Second–order and higher–order perturbations of travel time in isotropic and anisotropic media. *Stud. Geophys. Geod.*, **46**, 213–248.

Klimeš, L., 2003. Common ray tracing and dynamic ray tracing for S waves in a smooth elastic anisotropic medium. In: *Seismic Waves in Complex 3-D Structures, Report 13*, pp. 119–141, Dep. Geophys., Charles Univ., Prague, online at "http://sw3d.mff.cuni.cz".

Klimeš, L., 2004. Analytical one–way plane–wave solution in the 1-D anisotropic "simplified twisted crystal" model. *Stud. Geophys. Geod.*, **48**, 75–96.

Klimeš, L. and Bulant, P., 2004. Errors due to the common ray approximations of the coupling ray theory. *Stud. Geophys. Geod.*, **48**, 117–142.

Lakhtakia, A., 1994. Elastodynamic wave propagation in a continuously twisted structurally chiral medium along the axis of spirality. *J. Acoust. Soc. Am.*, **95**, 597–600, erratum: *J. Acoust. Soc. Am.*, **95** (1994), 3669.

Lakhtakia, A. and Meredith, M.W., 1999. Shear axial modes in a PCTSCM. Part IV: Bandstop and notch filters. *Sensors and Actuators A*, **73**, 193–200.

Pšenčík, I., 1998. Green's functions for inhomogeneous weakly anisotropic media. *Geophys. J. Int.*, **135**, 279–288.

Pšenčík, I. and Dellinger, J., 2001. Quasi–shear waves in inhomogeneous weakly anisotropic media by the quasi–isotropic approach: A model study. *Geophysics*, **66**, 308–319.

Thomson, C.J., Kendall, J-M. and Guest, W.S., 1992. Geometrical theory of shear–wave splitting: corrections to ray theory for interference in isotropic/anisotropic transitions. *Geophys. J. Int.*, **108**, 339–363.

Vavryčuk, V., 1999. Applicability of higher–order ray theory for S wave propagation in inhomogeneous weakly anisotropic elastic media. *J. Geophys. Res.*, **104B**, 28829–28840.

APPENDIX

The constant 3×3 real–valued orthogonal matrix E_{im}, describing rotation in 3-D space, has three independent components and may be expressed in terms of real–valued vector E_k. The direction of vector E_k specifies the axis of rotation, while the length

$$E = \sqrt{E_k E_k} \tag{A1}$$

of vector E_k specifies the angle of rotation about the half–axis given by vector E_k. The generating matrix of the rotation is

$$I_{ij} = \varepsilon_{ijk} E_k E^{-1} \quad , \tag{A2}$$

and the projection matrix onto the plane of rotation is

$$P_{ij} = \delta_{ij} - E_i E_j E^{-2} \quad . \tag{A3}$$

The generating and projection matrices satisfy relation

$$I_{ij} I_{jk} = -P_{ik} \quad , \tag{A4}$$

analogous to relation ii$=-1$ for the imaginary unit. Orthogonal matrix E_{ij} is then the exponential function of $I_{ij}E$,

$$E_{ij} = P_{ij} \cos(E) + I_{ij} \sin(E) + \delta_{ij} - P_{ij} \quad , \tag{A5}$$

i.e.

$$E_{ij} = \delta_{ij} \cos(E) + E_i E_j E^{-2} [1 - \cos(E)] + \varepsilon_{ijk} E_k E^{-1} \sin(E) \quad . \tag{A6}$$